Catchment-wide estimate of single storm interrill soil erosion using an aggregate instability index: a model based on geographic information systems

Christina Tsimi, Athanassios Ganas, Dimitrios Dimoyiannis, Spyros Valmis & Efthimios Lekkas

Natural Hazards
Journal of the International Society for the Prevention and Mitigation of Natural Hazards

ISSN 0921-030X
Volume 62
Number 3

Nat Hazards (2012) 62:863-875
DOI 10.1007/s11069-012-0114-8

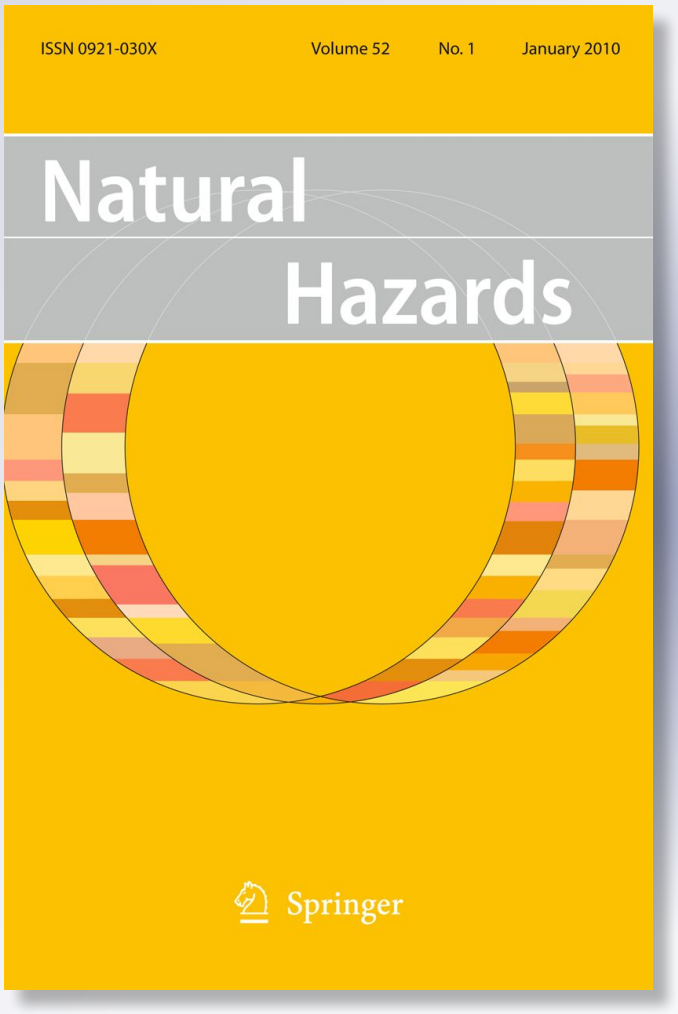

Springer

Nat Hazards (2012) 62:863–875
DOI 10.1007/s11069-012-0114-8

ORIGINAL PAPER

Catchment-wide estimate of single storm interrill soil erosion using an aggregate instability index: a model based on geographic information systems

Christina Tsimi · Athanassios Ganas · Dimitrios Dimoyiannis · Spyros Valmis · Efthimios Lekkas

Received: 4 March 2011 / Accepted: 9 February 2012 / Published online: 25 February 2012

Abstract The main objective of this paper is to estimate interrill erosion after rainfall in the basin of Mourganis river (442 km^2; Kalabaka province, Trikala prefecture, Thessaly, Greece). For the estimation of the interrill erosion, the method of Valmis et al. (1988) was used, in combination with Nearing et al. (1989). Input data of the algorithm include the slope angle of the ground surface, the rainfall, the ground cover type, the height of canopy, and the instability of ground of the study area. The spatial data were processed by standard GIS software. Soil samples were collected in the field to calibrate the model. The results comprise soil erosion maps for two specific rainfall scenarios. The first rainfall scenario refers to the most extreme rainfall in this catchment that happened on the 7/21/1959 with 48 mm/h. The second scenario is closer to average as the intensity rainfall is 3.54 mm/h. The total mass of eroded material ranges from 0.048 t/ha (assuming mean rainfall intensity) up to 3.5 t/ha (for the extreme scenario). We note that the western part of the Mourgani basin exhibits higher erosion than the eastern part.

Keywords Mourgani basin · Greece · Soil erosion · GIS

C. Tsimi
Department of Geography, University of the Aegean, Mytilene, Greece
e-mail: christinant@gmail.com

A. Ganas (✉)
Institute of Geodynamics, National Observatory of Athens, Lofos Nymfon, Thission, 11810 Athens, Greece
e-mail: aganas@gein.noa.gr

D. Dimoyiannis
National Agricultural Research Foundation, Larissa, Greece

S. Valmis
Agricultural University of Athens, Athens, Greece

E. Lekkas
Department of Geology and Geoenvironment, University of Athens, Athens, Greece

1 Introduction

Soil erosion is defined as a progress of detachment and transportation of soil material (Ellison 1947). The basic natural factors, which create the soil erosion by water, are the rainfall, the type of soil, and the geomorphology of area (Park et al. 1982). Erosion can be considered as a major environmental problem in Greece (e.g., Kosmas and Danalatos 1997; Valmis et al. 2005; Theocharopoulos et al. 2006; Myronidis et al. 2010), and increasing pressures are applied to authorities to provide quantitative estimates in view of rapid climate changes. In this study, geographic information systems (GIS) were used to establish an information data base to study a large catchment in central Greece and locate potential erosion areas using field analysis and modeling involving multiple layers. GIS characterized the catchment easily and efficiently.

The study region is the hydrological basin of the Mourganis River (Trikala, Greece, Fig. 1). The Mourganis River is a tributary of Pinios River. Mourgani basin's area is approximately 442 km^2, and river length is 47 km. The study area includes 26 settlements with a population of 6,208 inhabitants (EL.STAT 2001). In addition, the area includes a part of the national road Trikala—Grevena (15), as well as a part of the new motorway (E65), which is under construction. This area is one of the less-developed areas of Greece where population density is small and the local economy is primarily based on agriculture and farming.

The Mourganis River is directed east–west (flow is to the west) for about 30 km before turning south to join Pinios river (Fig. 1). The elevation of the study area ranges from 260 to 1,550 m. The slope map shows that high slopes are located in the west part of the area (<60%), whereas low slopes are located both in the riverbed and close to the settlement of

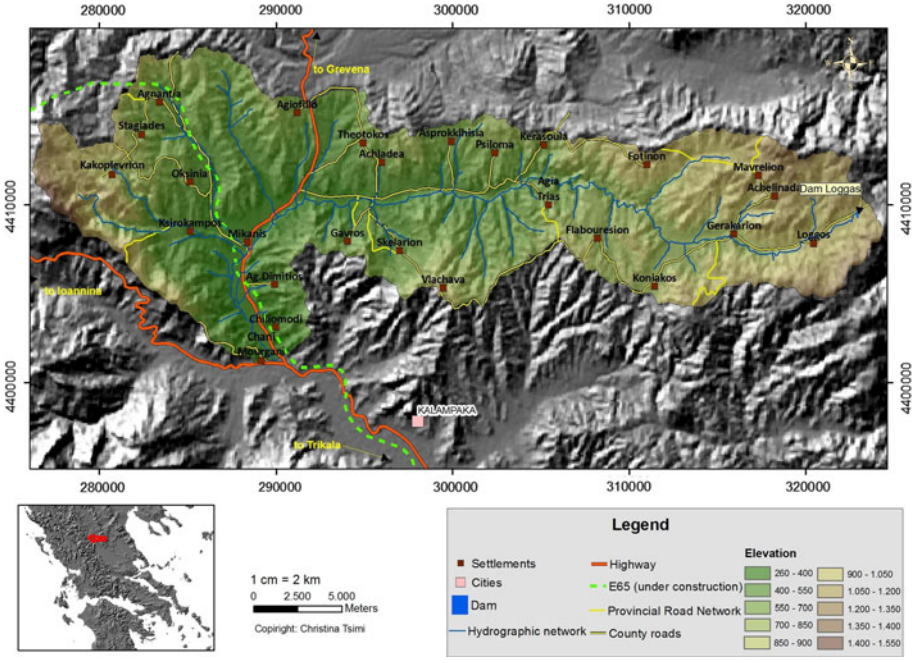

Fig. 1 Relief map of the study area (Mourganis catchment, Kalabaka, Greece). Map grid spacing is 10 km

Koniskos (Fig. 1; <5%). According to CORINE 2000 data (Büttner et al. 2004), a large part of the study region is covered with forests (29.6%) and agriculture areas (29.4%). Furthermore, the natural grasslands cover 11.8%, and the sclerophyllous vegetation covers 11.6%. A small area (0.4%) is covered with urban fabric.

In terms of geology, the Mourganis basin is located in the Mesohellenic sedimentary trough that was formed during the Oligocene epoch—early Miocene (30–20 Ma; Brunn 1956; Papanikolaou et al. 1986; Zelilidis et al. 2002). The 1:50000 geology map series (IGME 1980) shows that the lithology of the eastern part is mainly bedrock: gneises, actinolite schists, and mica schists of lower Paleozoic age. The central part of the Mourgani Basin is extensively covered with molassic sediments of marine origin (Fig. 2). There are three molassic sediment series. The *Pentalofon* series, in the western part, is composed by conglomerate, sandstone, and marl. The *Tsotili* series, in the central and eastern part of study region, is composed by conglomerate, sandstone, and marl, while a small part is also composed by sandstone and marl. The third series is the *Heptachorion* series, in the central and western part of study region. This series is composed by sandstone and marl, also a small part is composed by conglomerate. The lithology in the western part consists of ophiolites (ultrabasic igneous rocks).

According to our own field work, the soil erosion that can be identified in the Mourganis basin is mostly erosion at layers (*Interrill*): raindrops striking exposed soil detach the soil particles and splash them into the air and into shallow overland flows. Erosion at layers appears between small rills, mainly caused by rainfall, flow and transfer of soil molecules through the hydrographic network caused by the plash of raindrops, and the shallow ground flow (Hadley et al. 1985; Meyer and Harmon 1989). Extensive research has been conducted to calculate the rate of erosion at rills, which was based on laboratory

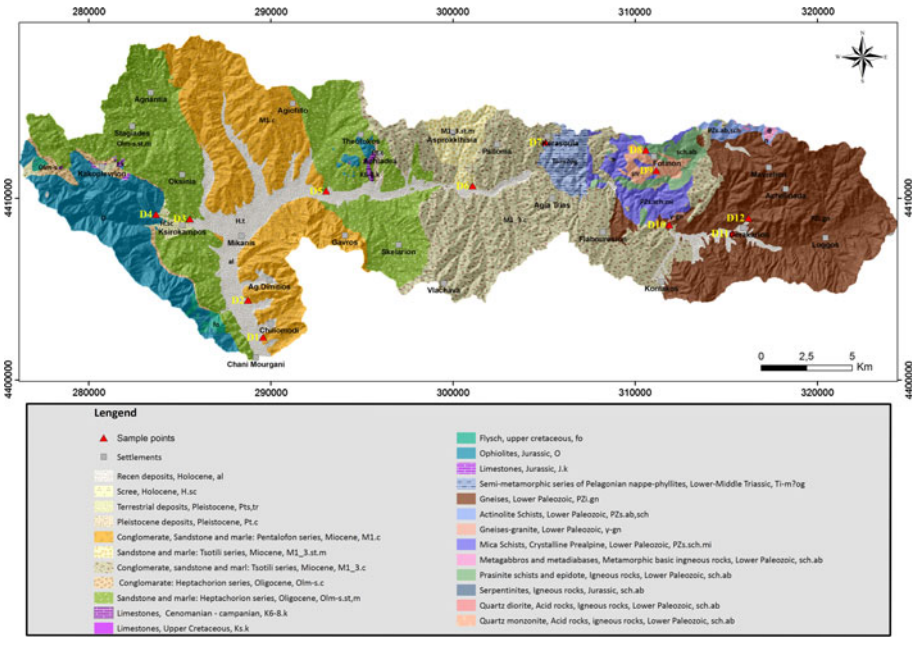

Fig. 2 Geological map of the Mourganis basin. The map was constructed by rectification and mosaicking of three (3) 1:50000 map sheets of IGME. Red triangles indicate sample locations reported in Table 2

experiments using rainfall simulators. The major factors considered for the calculation of the erosion rate are the rainfall intensity and slope. The core of the method is the estimation of the soil instability index β (Valmis et al. 2005; Dimoyiannis et al. 2006). β is a composite parameter that embodies many soil properties affecting structural stability, such as texture, organic matter content, sesquioxides content, etc. Thus, it can be considered that it successfully describes the vulnerability of soils to erosion, accounting for soil variability.

2 Materials and methodology

Geographic information systems are powerful tools used to collect, store, retrieve, process, model, and display spatial data from the real world for soil erosion studies. The use of GIS in this field is a recent topic (e.g., Petersen et al. 1998), mainly its application in erosion modeling. The software used was *ArcGIS v.9.3* for Windows. Available analogue data included three 1:50000 scale map sheets of the Hellenic Army Geographical Service (HAGS) and three 1:50000 scale geology maps from the Institute of Geological and Mineral Exploration of Greece (IGME). The GIS database included the following geospatial data: land elevation, cities, river network, road network, geology, and land use. The following spatial features were digitized: a) catchment boundaries (total number 56), b) streams c) geology formations, d) elevation contours at 20-m intervals, and e) elevation points (usually benchmarks on mountain peaks). The Greek national projection system (EGSA87; ASPRS 2002) was used for all data, and a 4-pixel snapping tolerance during digitization process was accepted. The Mourganis basin can be classified as a six-class basin according to Strahler's classification (Strahler 1952).

The Digital Elevation Model (DEM) was constructed by combining elevation information from photogrammetrically extracted contours (20-m interval; from HAGS maps; procedure and product accuracy is described in Ganas et al. 2005) and elevation points (benchmarks from the 1st-order trigonometric network of Greece). Natural Neighbour (Sibson 1981) was the spatial interpolation method used with pixel size 30 m $\times$ 30 m. The slope was calculated from the DEM using a *Third-order finite difference* algorithm from Horn (1981) and window size 3 $\times$ 3 pixels. Jones (1998) compared the slope algorithms and concluded that Horn's algorithm is better to calculate slope at surfaces with rough relief.

2.1 Rainfall

It is assumed that maximum rainfalls follow a frequency of distribution of extreme values (Gumbel 1954). Gumbel (1954) suggested a relation of exponential probability based on the extreme values. In this research, a distribution Gumbel—type 1 (method of moments) was used. In our statistical analysis, 24 h/day rainfall measurements for the period 1951–1997 were used. Those data were collected at Ayiofillo meteorological station (Ministry of Public works) located inside the Mourganis basin (location in Fig. 1). It was found that daily rainfalls ranging from approximately 35–48 mm have high probability to occur, over 50%, and the return period is between 1 and 2 years. Moreover, rainfalls that range from 50 to 65 mm have a lower probability of occurrence (20–30%), and the return period is 2–5 years. Rainfalls with $\sim$70–80 mm have return period 10 years and a lower probability of occurrence (Fig. 3). The rainfall occurred in 7/21/1959 is extraordinary because it has both high intensity (48.6 mm/h) and rainfall (77.9 mm) (Table 1).

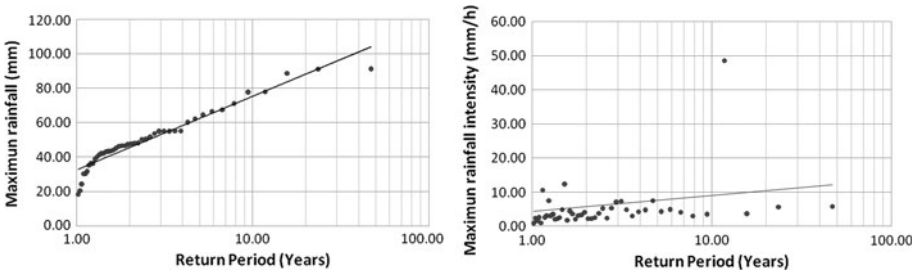

Fig. 3 (*left*) Variation of maximum 24-h rainfall with the return period for the Ayiofillo meteorology station. (*right*) Variation of maximum 24-h rainfall intensity with the return period for the Ayiofillo meteorology station

Table 1 Statistics for the maximum 24-h rainfall (mm)

Mean	50.31
SD	16.98
Min	18.3
Max	91.3

Data from Ayiofillo station (see Fig. 1 for location). Max value was observed on November 1953

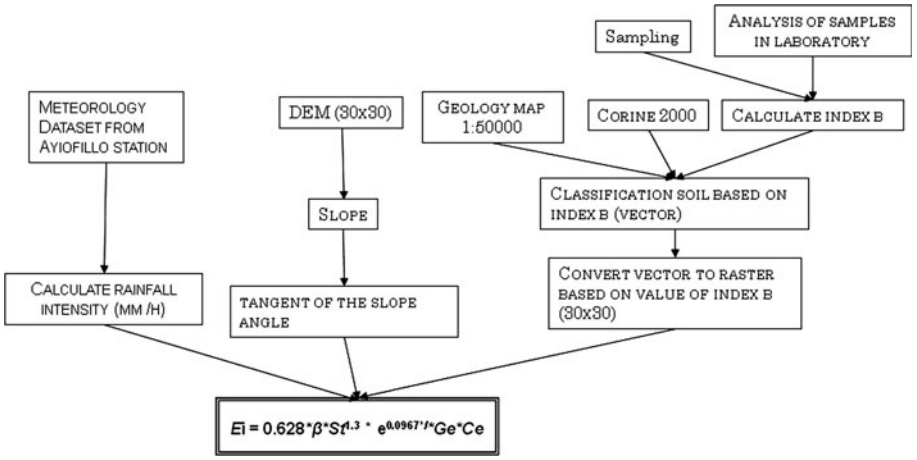

Fig. 4 Flow diagram of data and methods used in the Mourganis GIS to estimate the interrill erosion rate (E_i)

2.2 Soil erosion

In this research, for the estimation of the interrill erosion the method of Valmis et al. (2005) was used, in combination with Nearing et al. (1989). Valmis et al. (2005) proposed that soil detachment by raindrop impact, which strongly depends on aggregate stability, is the principal erosion process controlling interrill erosion (Bradford and Huang 1996). This method uses the following spatial and climatic data: ground slope, rainfall, ground cover, canopy cover, and ground stability at the study area. The flow chart of the algorithm is presented in Fig. 4.

$$E_i = 0.628 * \beta * S_t^{1.3} * e^{0.0967*I} * G_e * C_e \quad (1)$$

E_i Interrill erosion rate (kg/m^2)
B Instability index
I Rainfall intensity (mm/h)
S_t Tangent of the slope angle
G_e Effect of the ground cover

$$G_e = e^{(-2.5g_i)} \quad \text{(Nearing et al. 1989)} \quad (2)$$

where g_i is the fraction of surface that is covered by ground vegetation or plant remnants

C_e Effect of the canopy cover

$$C_e = 1 - F_{c*}e^{-0.34H_c} \quad \text{(Nearing et al. 1989)} \quad (3)$$

where F_c is the fraction of ground that is protected from canopy cover, and H_c is the height of the canopy (m).

The tangent of the slope angle was estimated from function (4). This function calculates the slope from DEM, extracts the pixels that value $\geq 4°$, and calculates the tangent of the slope angle to a new raster dataset with pixel size 30 m × 30 m.

$$\text{Tan}\ ((((\text{[slope]} > = 4)\ \text{IN}\{1\}) * \text{[slope]})\ \text{DIV DEG}) \quad (4)$$

Information about indexes C_e and G_e was obtained during field research in July 2009 according to the bibliography (Cook and Stubbendieck 1986; Jennings et al. 1999). As erodible areas are considered those covered with: (a) canopy with average cover 20% ($F_c = 0.2$) and average height of 2.5 m ($H_c = 2.5$) and (b) vegetation or plant remnants with average cover 40% ($g_i = 0.40$). Moreover, the erosion of the areas covered with forest and alluvial deposits close to Mourganis River (Fig. 1) was not estimated due to near zero slope steepness (between 0° and 4°), that is, it is assumed as areas with zero interrill erodibility. The area of those lowlands is about 62 km^2, or 14% of the total catchment area. The Index β (Valmis et al. 1988; Dimoyiannis et al. 1998) was estimated from the following function:

$$\beta = [\log(W_a - W_s) - \log(W_i - W_s)]/2 \quad (5)$$

W_a The dry mass of the initial sample (gr)
W_s The dry mass of the sand-sized primary mineral particles (gr),
W_i The dry mass of the materials remaining on the sieve after the soaking (gr)

For ideal, perfectly stable aggregates (100% of the initial sand content-corrected dry mass of aggregates is retained on the sieve), β takes the lowest value, for example, $\beta = 0$. In the case of a completely unstable soil (1% of the initial sand content-corrected dry mass of aggregates is retained on the sieve), $\beta = 1$. For the estimation of Index β, twelve (12) soil samples were collected from the study region on July 23, 2009 (the sample locations can be seen in Fig. 2). In Greece, the most intense storm events occur in the period from late-spring to mid-fall so our sampling timing can be considered suitable for realistic erosion estimates. Sampling was conducted in order to collect material from all the possible geological formations combined with the land uses as they were classified by CORINE 2000 (Büttner et al. 2004). The analysis of calculating Index β was conducted in

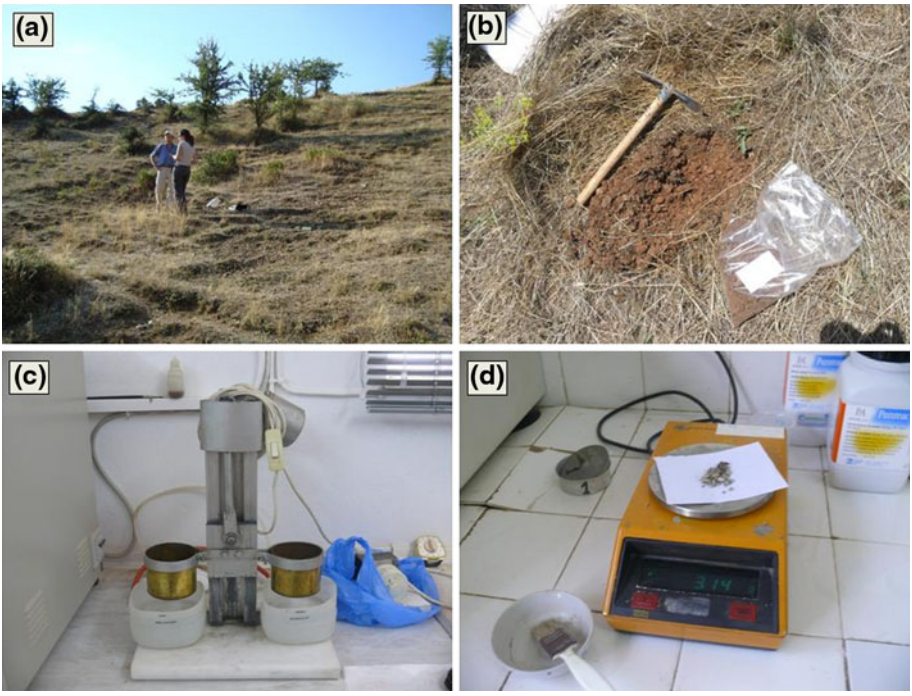

Fig. 5 **a** Interrill erosion in the study region (location near 39.81° N, 21.80°E, 7/23/2009; sample D10 on gneiss) **b** Field photograph of sampling point D4 (location 39.81°N, 21.47°E; rock type peridotite), **c** Photograph showing the disk movement for the wet sieving of soil samples, **d** Photograph showing the W_s estimation

the laboratory of National Agricultural Research Foundation (N.AG.RE.F.; Fig. 5) in Larissa (central Greece). The technique of wet sieving was applied for 4 min per sample. The results are reported in Table 2 with values ranging 0.019–0.421. Samples with high β originated from conglomerate and sandstone areas. Then, the *intersect* algorithm from ArcToolbox (in ARC GIS) was used to create a new vector (polygon) dataset that has information regarding the geology and the land use for every polygon. Based on this dataset, we classified index β. Finally, this dataset was converted from vector to raster based on index β with pixel size 30 m $\times$ 30 m (see Fig. 6).

The index E_i was calculated for two cases of rainfall intensity. The first case refers to the most extreme rainfall which happened in our study area (7/21/1959), where the rainfall intensity is 48.6 mm/h, and the height of rainfall is 77.9 mm. The second case has a small return period and high probability of occurrence for rainfall up to 40 mm. Based on the method of moments, the rainfall intensity is 3.54 mm/h, the probability of occurrence is 74.5%, and the return period is 1.31 year.

3 Results and discussion

In the most common case of rainfall intensity of 3.54 mm/h, the highest value of soil erosion is 0.11 kg/m^2 (Fig. 7) and occurs in western sub-basins of the Mourganis river. The

Table 2 Experimental results, individual and mean values of the instability index β

a/a	Sample	Lon.	Lat.	Geology	Initial weight	(W_a)	W_i (1)	W_s (1) SAND	β_1	W_i (2)	W_s (2)	β_2	β
1	D1	21.546	39.748	Conglomerate	7.88	7.80	3.68	2.94	0.409	3.84	3.22	0.434	0.421
2	D2	21.535	39.766	Sandstone	7.74	7.58	6.97	2.77	0.029	7.11	3.14	0.024	0.027
3	D3	21.497	39.805	Sandstone	7.91	7.63	3.70	0.30	0.167	3.49	0.39	0.184	0.176
4	D4	21.475	39.807	Ophiolites	8.01	7.70	6.80	3.89	0.059	6.68	3.82	0.066	0.062
5	D5	21.584	39.821	Conglomerate	8.01	7.72	2.67	0.16	0.239	2.38	0.22	0.270	0.255
6	D6	21.677	39.825	Conglomerate	7.98	7.83	7.17	3.45	0.035	7.10	3.14	0.037	0.036
7	D7	21.723	39.848	Conglomerate	7.98	7.85	6.94	2.83	0.043	6.69	2.81	0.057	0.050
8	D8	21.788	39.845	Schist	8.00	7.80	7.21	5.03	0.052	7.19	5.42	0.064	0.058
9	D9	21.795	39.835	Schist	8.02	8.00	7.87	7.41	0.054	7.85	7.31	0.053	0.054
10	D10	21.804	39.809	Gneiss	8.00	7.94	7.48	4.57	0.032	7.50	5.76	0.049	0.040
11	D11	21.845	39.805	Gneiss	8.00	7.99	7.84	7.18	0.044	7.83	7.34	0.061	0.053
12	D12	21.855	39.813	Gneiss	8.01	7.98	7.92	7.39	0.023	7.96	7.66	0.014	0.019

The sampling points can be seen in Fig. 2

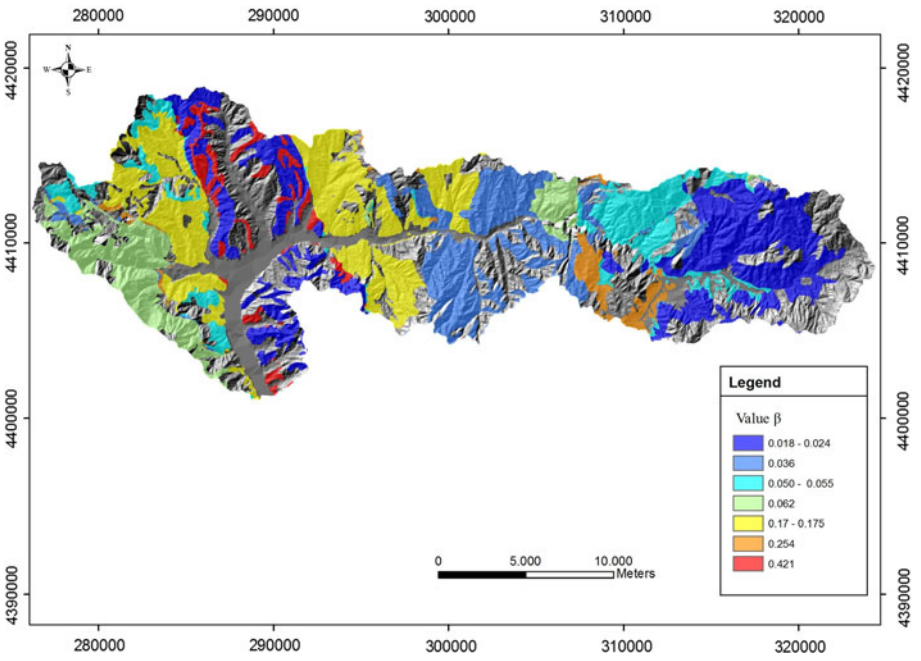

Fig. 6 Map of Mourganis basin showing spatial distribution of β-index. High β values indicate large soil erodibility

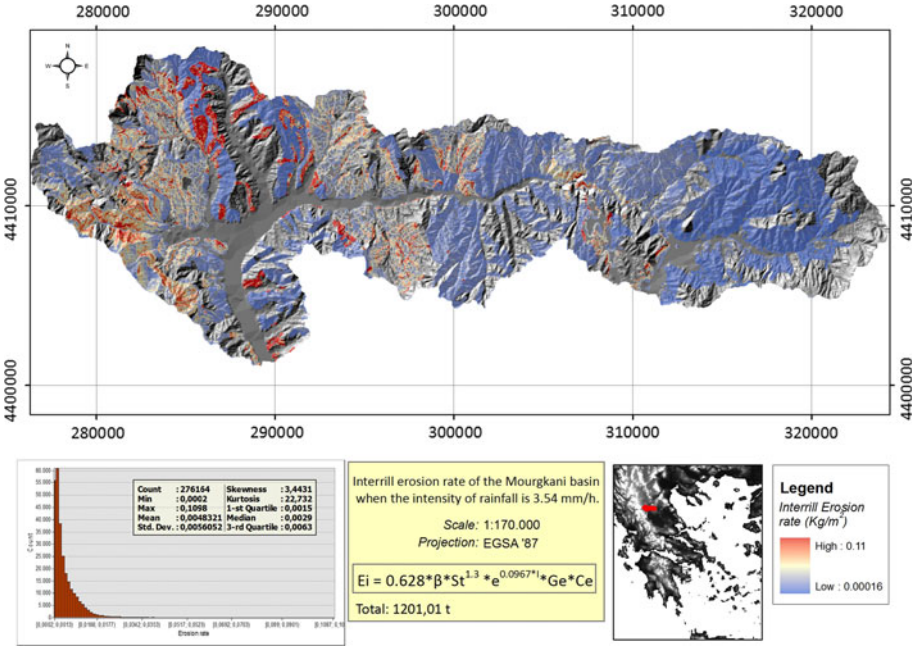

Fig. 7 Map of single storm interrill soil erosion of the Mourganis basin assuming rainfall intensity of 3.54 mm/h

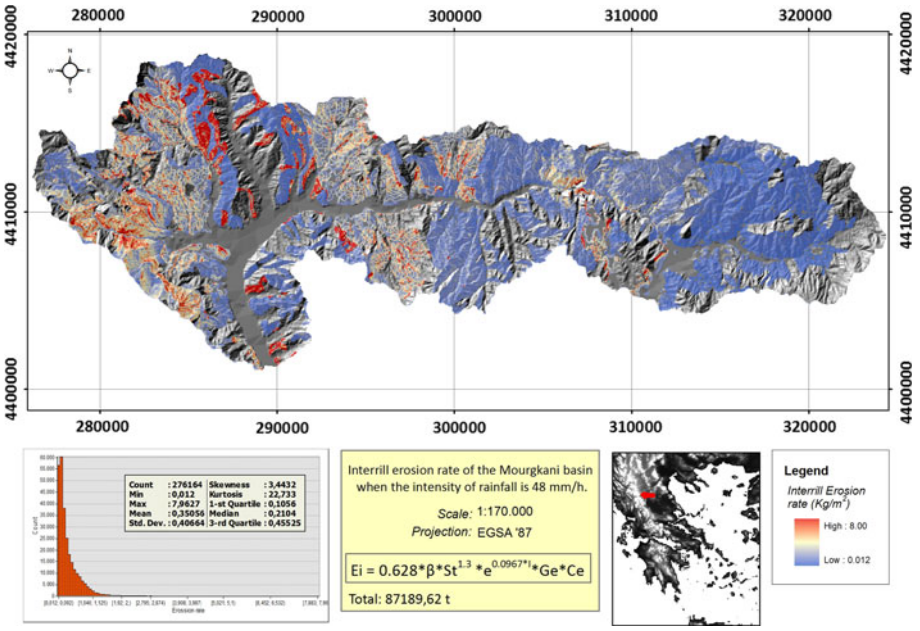

Fig. 8 Map of single storm interrill soil erosion of the Mourganis basin assuming rainfall intensity of 48 mm/h

22% of the basin area exhibits erosion values ranging from 0.0013 to 0.017 kg/m^2. The total mass of eroded material is estimated at 1,201,014 kg, or 1,201 tonnes (0.048 t/ha). For the extreme rainfall case (Fig. 8), the highest erosion rate is 8 kg/m^2, and the mean value is 0.35 kg/m^2. The total mass of eroded material is estimated at 87,130,224 kg (87,130 tonnes; 3.5 t/ha) or 73 times larger. This interrill sediment loss is at the low end of the range of values obtained from Dimoyiannis et al. (2006) for cultivated soils in central Greece (1.6–49.3 t/ha; Dimoyiannis et al. 2006, Table 1). Larue (2001), working on sandy soils under cultivation in the western Paris basin, measured some 0.15–0.2 t/ha interrill soil losses during the month following sowing. These losses, compared with our estimation for Mourganis catchment, are 3–5 times higher for common-rainfall events and one order of magnitude less for extreme rainfall events; however, they also concern cultivated soils and have been recorded for a time span of a month. It is well known that cultivated soils are especially susceptible to water erosion.

A quick assessment of uncertainties in the above calculations included the widening of the values allowed for the parameter F_c (canopy cover) in Eq. 3. The calculations were repeated for $F_c = 0.1$ (i.e., 10% of the pixel is covered by canopy) and $F_c = 0.3$. The results in the extreme rainfall case are in range ±20% of our initial estimate (3.5 t/ha). For other researchers who might wish to follow this methodology, potential sources of error include a) the slope angle accuracy and b) the ground cover conditions. The first is a function of map scale and algorithm used in slope calculation. It is suggested that the 1:50000 scale (used in this study) is a good analogue for local basin studies. The second error source (ground cover) is affected by the assessment in the field and by land cover information.

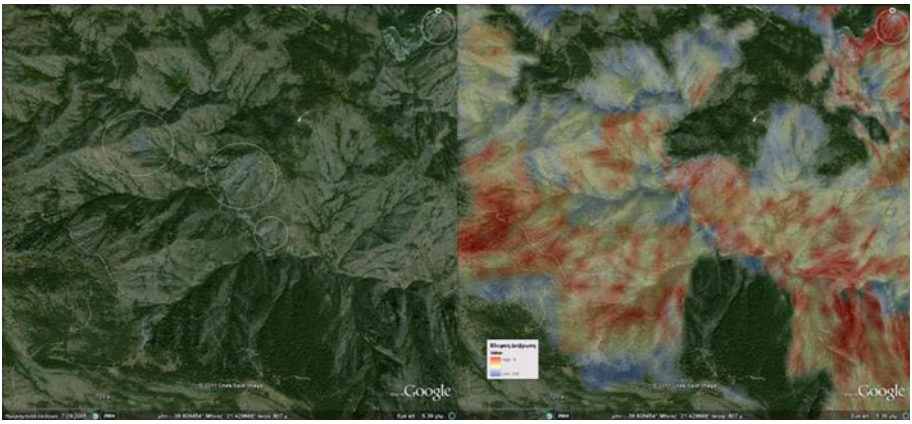

Fig. 9 Google Earth imagery of western part of the Mourganis basin showing high erosion model results (*right*) in areas with earth slides (*left*, *white circles*). A rainfall intensity scenario of 48 mm/h is assumed

The results from the soil erosion model were compared (in a qualitative sense) with a photo-interpretation from the Google Earth™ image, in the western sub-basins (Fig. 9, west of Ayiofyllo, and south of village Kakoplevrion; Fig. 1). In this area, the Google image is a high-resolution satellite image obtained by Digital Globe on March 27, 2003 (last checked on November 9, 2011; Fig. 9 left). In areas where a high erosion rate is predicted (Fig. 9 right), there are landforms resulting from high erosion (debris flows, etc.), as well as numerous landslides. Here, protective measures are needed, especially in terms of maintenance and enhancement of vegetative cover. In terms of sediment deposition, it is easy to identify on Google Earth imagery large areas of recent deposits at both river banks of Mourganis, supporting the idea that eroded material is transported downstream.

The proposed methodology is useful for the following purposes: (1) To implement a methodological approach (Fig. 4) and capacity building program, for supporting plans to manage land degradation and soil productivity in mountainous catchments in Greece, (2) to provide the planners and decision makers with a realistic thematic map of river catchments (erosion risk map, Fig. 6) (3) to provide the planners—engineers and local authorities with GIS tools for acquiring knowledge on causes and effects of soil erosion so as to provide quantitative estimates in view of rapid climate changes, and (4) to contribute toward the production of guidelines and recommendations for soil erosion monitoring.

4 Conclusions

1. Soil erosion is a surface process that can be evaluated, as well as monitored using GIS techniques. A methodology based on digital analysis of spatial and climatic data (elevation, land cover, geology, etc.) was applied in order to estimate soil erosion on a basin-wide scale for the Mourganis catchment, Kalabaka area, central Greece, where the main form of the soil erosion occurring is that of interrill erosion.
2. Our study used field data (soil samples) to calculate the soil instability index β (Fig. 6) to calibrate the erosion model. The total mass of eroded material ranges from 0.048 t/ha (assuming mean rainfall intensity of 3.54 mm/h) up to 3.5 t/ha (for the extreme scenario, 48 mm/h).

3. These values are relatively low in comparison with sediment loss from cultivated soils in central Greece.
4. The most vulnerable areas in the catchment are the western ones. Here, protective measures are needed, especially in terms of maintenance and enhancement of vegetative cover. For the efficient implementation of the above methodology, which is not appropriate for studying rill or gully erosion, care must be taken in describing vegetative cover, since it varies seasonally.

Acknowledgments We thank the Ministry of Environment and Public Works (Athens, Greece) for providing rainfall data for Ayiofyllo station. The study was partly financed by the Earthquake Planning and Protection Organisation of Greece and the National Observatory of Athens. We thank the Global Scale Ltd. (Cyprus) for technical support. We also thank our colleagues Nikos Soulakellis and Yannis Fountoulis for comments.

References

ASPRS (2002) http://www.asprs.org/resources/grids/12-2002-hellenic.pdf

Bradford JM, Huang C (1996) Splash and Detachment by Waterdrops. In: Agassi M (ed) Soil erosion, conservation and rehabilitation. Marcel Dekker, New York, pp 61–76

Brunn J (1956) Contribution à l'étude du Pinde septentrional et d'une partie de la Macédoine occidentale. Annales Géologiques du Pays Helléniques 7:1–358

Büttner G, Feranec J, Jaffrain G, Mari L, Maucha G, Soukup T (2004) The CORINE Land Cover 2000 Project. EARSeL eProceedings 3(3):331–346

Cook CW, Stubbendieck J (1986) Range research: basic problems and techniques. Society for Range Management. Denver, Colorado, USA. http://www.eea.europa.eu/data-and-maps/data/corine-land-cover-2000-clc2000-seamless-vector-database

Dimoyiannis D, Tsadilas C, Valmis S (1998) Factors affecting aggregate instability of Greek agricultural soils. Commun Soil Sci Plant Anal 29:1239–1251

Dimoyiannis D, Valmis S, Danalatos NG (2006) Interrill erosion on cultivated Greek soils: modeling sediment delivery. Earth Surf Process Landf 31:940–949

Ellison WD (1947) Soil erosion studies, part I. Agric Eng 28(4):145–146

Ganas A, Pavlides S, Karastathis V (2005) DEM-based morphometry of range-front escarpments in Attica, central Greece, and its relation to fault slip rates. Geomorphology 65:301–319

Gumbel EJ (1954) Statistics of Extremes. Colombia University Press, New York

Hadley RF, Lal R, Onstand CA, Walling DE, Yair A (1985) Recent developments in erosion and sediment yield studies. Report Unesco(IHP), Paris

Horn BKP (1981) Hill shading and the reflectance map. Proc IEEE 69(1):14–47

IGME (1980) Geological map of Ayiofyllo. Scale 1(50):000

Jennings SB, Brown ND, Sheil D (1999) Assessing forest canopies and understorey illumination: canopy closure, canopy cover and other measures. Forestry 72(1):59–73

Jones K (1998) A comparison of algorithms used to compute hill slope as a property of the DEM. Comput Geosci 24(4):315–323

Kosmas C, Danalatos N (1997) The effect of land use on runoff and soil erosion rates under Mediterranean conditions. Catena 29:45–49

Larue JP (2001) Runoff and interrill erosion on sandy soils under cultivation in the western Paris basin: mechanisms and an attempt at measurement. Earth Surf Process Landf 26(9):971–989

Meyer LD, Harmon WC (1989) How row-side slope length and steepness affect interrill erosion. Trans ASAE 32:639–644

Myronidis DI, Emmanouloudis DA, Mitsopoulos IA et al (2010) Soil erosion potential after fire and rehabilitation treatments in Greece. Environ Model Assess 15(4):239–250

Nearing MA, Foster GR, Lane LJ, Finker SC (1989) A process-based soil erosion model for USDA-Water Erosion Prediction Project technology. Trans Am Soc Agric Eng 32:1587–1593

Papanikolaou D, Lekkas E, Mariolakos I, Mirkou R (1986) Contribution to the geodynamic evolution of the Mesohellenic basin. Bull. Geol. Soc. Greece, XX, pp 17–36

Park SW, Mitchell JK, Bubenzer GD (1982) Splash erosion modeling: physical analyses. Trans Am Soc Agric Eng 25:357–361

Petersen GW, Nizeyimana E, Evans BM (1998) Application of geographic information systems in soil degradation assessment. In: Lal R, Blum WH, Valentine C, Stewart BA (eds) Methods for assessment of soil degradation. CRC Press, Washington, pp 377–391

Sibson R (1981) A brief description of natural neighbor interpolation. In: Barnett V (ed) Interpreting multivariate data. Wiley, Chichester, pp 21–36

Strahler AN (1952) Dynamic basis of geomorphology. Geol Soc Am Bull 63:923–938

Theocharopoulos SP, et al (2006) Modeling soil erosion in central Greece. Abstract presented in the 18th world congress of soil science (July 9–15, 2006)

Valmis S, Kerkides P, Aggelides S (1988) Soil aggregate instability index and statistical determination of oscillation time in water. Soil Sci Soc Am J 52:1188–1191

Valmis S, Dimoyiannis D, Danalatos NG (2005) Assessing interrill erosion rate from soil aggregate instability index, rainfall intensity and slope angle on cultivated soils in central Greece. Soil Tillage Res 80(1–2):139–147

Zelilidis A, Piper DJW, Kontopoulos N (2002) Sedimentation and basin evolution of the Oligocene-Miocene Mesohellenic basin, Greece. AAPG Bull 86(1):161–182